Journal of Materials Chemistry A

Accepted Manuscript

ROYAL SOCIETY OF CHEMISTRY

www.rsc.org/materialsA

Journal Name

RSCPublishing

COMMUNICATION

Impact of Large-Scale Meso- and Macropore Structure in Adenosine-derived Affordable Noble Carbon on Efficient Reversible Oxygen Electrocatalytic Redox Reaction

Cite this: DOI: 10.1039/xoxxoooooox

Received ooth January 2012,
Accepted ooth January 2012

DOI: 10.1039/xoxxoooooox

www.rsc.org/

K. Sakaushi,[a, ‡, *] S. J. Yang,[a] T.-P. Fellinger,[a] and M. Antonietti[a]

In this report, we delineated a successful synthesis of a high performance and affordable Adenosine-derived noble carbon cathode for LOBs with bifunctional electrocatalytic activity and showed that the pore structure of cathode is a key feature to control the electrochemical performance of this electrochemical system.

Mastering functions of energy material is one of the most challenging topics in modern science in order to achieve a stable energy supply.[1] Especially economically feasible rechargeable electrochemical energy storage is one of the most urgent requirements to realize a society equipped with an electrical grid system where renewable energies are a major component.[2, 3] An important enrollment of future rechargeable battery with multiple function is within electronic vehicles (EVs). EVs should be used to store green energy in peak times supplied from the above grid system, and it relies on materials development for cost-effective but high performance electrodes, electrolytes and other components to sum up to a performance comparable to the current combustion engines. Rechargeable metal-air battery technology is expected to be able to match those expectations.[4, 5] However, already development of rechargeable Lithium-Oxygen Batteries (RLOBs) is hampered by its complicated electrochemical reactions.[6-10] Recent results clarified the importance of electrolyte in RLOB systems,[9, 10] but research on the novel porous cathodes is of similar importance to improve electrochemical properties in general.[11-16] The pore structure is indeed important for a RLOB system not just for oxygen supply, but for fundamental understanding of electrochemical reactions.[17, 18] Those electrochemical reactions initially occur at the interface between catalytic cathode surface and O_2-saturated electrolyte as a starting trigger,[5, 9, 10] and then the electrochemical growth of the (insulating) lithium peroxide (Li_2O_2) on the cathode surface drives further space-temporal development of the materials structure. Here, we show that the pore structure of cathodes can obvious direct this structure formation and has thereby a significant effect on specific capacity and rechargebility of lithium-oxygen cells. We vary here the pore structures of N-doped carbons, so-called noble carbons. In this report, we show that noble carbons synthesized from adenosine being a model for a sustainable precursor as such exhibit a high catalytic activity in both the oxygen reduction and evolution reaction, comparable to metal-based catalysts.

The promising properties in catalytic reactions of doped carbons are not new as such.[19-26] In our previous report we described mesoporous Noble Carbons (NCs), constituted mainly of the elements C and N and therefore being sustainable and affordable, to be an efficient bifunctional catalyst working for both oxygen reduction reaction (ORR) and oxygen evolution reaction (OER) in non-aqueous RLOB systems.[27] The RLOB cell using ionic liquid (IL) based porous NC cathode exhibited a comparably low overpotential during charge and discharge cycles. In the OER reaction, the mesoporous NC cathode already showed an overpotential of "only" 0.45 V, a performance comparable to cathodes using expensive noble metal catalysts such as Au.[28] Although still there is a problem on the reactivity during both charge and discharge reaction,[29-31] recent research using differential electrochemical mass-spectrometers confirmed that carbon-based cathodes are one of the most promising catalysts for reversible charge-discharge reaction of RLOBs.[8] Therefore, we intend here to perform further investigation on large-scale meso/macroscopic pore structures to improve rechargebility and cycling life by controlling the porous structure of the noble carbon cathode. This was performed by applying salt melt synthesis, which can enable to synthesize materials with controlled pore structures.[32] Adenosine was selected as a clean model for DNA-derived sustainable precursors towards materials with electrocatalytic properties as good as IL-based noble carbons. The resulting adenosine-based porous noble carbons (APNCs) have a different large-scale meso- and macroporosity without any change of microporosity and chemical structure. The pore structure of NCs has indeed a significant effect on the specific capacity and rechargebility of RLOB cells: The APNC showing the best performance within our sample set has a high amount of large-scale meso- and macroporosity. With larger pore volume contributed from macropores the RLOB cell shows a

lower overpotential and a high specific capacity, while the APNC having less macropores only showed low specific capacity.

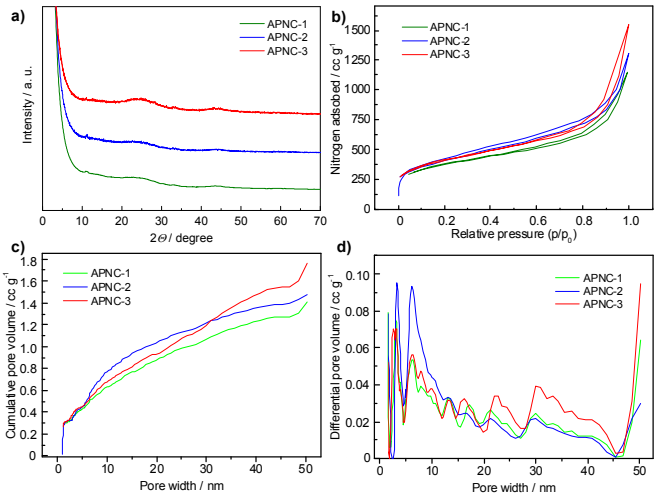

Figure 1. Physical characterizaion of APNCs. (a) XRD patterns. (b) N_2 isotherms. (c) Pore width vs. Cumulative pore volume diagrams. (d) Pore size distributions.

Table 1. N_2 sorption data for APNCs

Sample	BET Surface Area (m^2/g)	Micropore Volume (cc/g)	Mesopore Volume (cc/g)	Total Pore Volume (cc/g)
APNC-1	1321	0.308	1.106	1.778
APNC-2	1456	0.323	1.157	2.021
APNC-3	1476	0.320	1.440	2.387

The APNCs were synthesized adding adenosine to a binary salt mix (a combination of KCl and $ZnCl_2$ with the mass ratio of 1.00 to 1.75). The "salt-melt synthesis" as a template procedure enables to control the pore volume in carbonaceous materials with high specific surface area by just changing the ratio of starting material and a salt.[32] The technique was applied to have a series of N-doped carbons with the same micropore volume, but different controlled meso- and macropore structures. Adenosine was chosen as the carbon source because it provides a high carbonization yield with high nitrogen content and a favourable oxidation stability of the final material. Adenosine as such is rather expensive but is to be understood as a model for digested bacterial DNA, a comparably cheap, sustainable product of fermentation which allows scalability of the process. We chose three ratio of adenosine and salts (A:S) as A:S = 5:1 (described as APNC-1), A:S = 5:2.5 (APNC-2), and A:S = 5:5 (APNC-3). Then, the samples were carbonized at 1000 °C for two hours, washed with distilled water overnight, and obtained three different APNCs. Although the X-ray diffraction (XRD) patterns of APNCs show weak diffraction intensity which to our experience suggest nanometer carbon wall thickness and high porosity, the broadened (002) peak indicated graphitized character of resultant carbon materials (Figure 1a). The results of elemental analysis (EA) showed that N-content of all APNCs is around 5 % (Table S1). The chemical structures of doped nitrogen in all three samples were confirmed by X-ray photoemission spectrometer (XPS). The results of XPS showed that the chemical structures of nitrogen in three samples are almost same (Figure S1). Indeed, Raman spectroscopy also revealed that the physic-chemical nature of all three samples is similar (Figure S2). The surface textural characteristics of the APNCs were quantified by measuring the N_2 isotherms at cryogenic condition (77 K). (Figure 1b-d and Table1). Overall, the N_2 isotherms of the APNCs exhibited combined characteristics of typical type I and IV materials. A steep increase in low pressure was observed, followed by a moderate slope at intermediate pressure accompanied by a small desorption hysteresis and a dramatic increase near at 1.0 of relative pressure. These properties indicated the combined presence of micro-, meso-, and macrosized pores. From Table 1 and pore size distribution (Figure 1c and d), extracted from the isotherms using non-local density functional theory (NLDFT), clear differences in the pore structure of the samples can be found.[33] As the amount of salt template increased, large-scale meso- and macroporosity of the resulting carbons, could form without notable changes of microporosity and the specific surface area (Fig. 1b,c). Scanning electron microscopy (SEM) and transmission electron microscopy (TEM) observation revealed that APNC-1 exhibit an apparently smooth surface, i.e. macropores are absent, while APNC-3 shows a morphology of interconnected carbon nanoparticles with interstitial large-scale meso-, and macropores (Figure 2 and Fig S3). This large-scale mesoporosity and macroporosity of APNC-3 (Fig 1d, 2c, S3) provides transport channels for improved contact with oxygen, but also enabling the rapid long range transport of electrolyte ions.

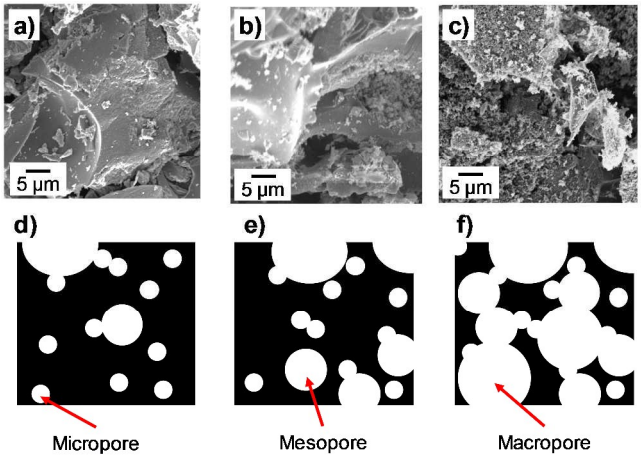

Figure 2. SEM images (a-b) and schematic illustrations (d-e) of APNCs

Together with XRD, SEM, TEM, EA, XPS, and Raman results, these observations demonstrate that the pore characteristics of the resulting carbons are easily tuned by controlling the amount of used salt while maintaining the physical-chemical wall structure. The following electrochemical properties are thereby mainly affected by the pore structure of the samples.

The charge-discharge curves of APNCs in a LOB set-up indicate that there is a strong impact of porosity on electrochemical performance. We applied 2.3 V vs. Li/Li^+ as the lower cut-off voltage and 4.0 V vs. Li/Li^+ as the upper cut-off voltage. The upper cut-off voltage was chosen to minimize the irreversible specific capacity which caused by side reactions from the electrolyte decomposition as previous researches clearly shown the CO_2 evolution above 4.0 V vs. Li/Li^+ by quantitative differential electrochemical mass spectroscopy.[29, 34, 35] A current density of 100 mA/g was selected for this

experiment. Our electrochemical data of APNCs are summarized in Table 2. The charge-discharge curves of APNCs show that already the bare N-doped carbon materials without any metal exhibit bifunctional catalytic properties for both oxygen reduction reaction and oxygen evolution reaction at discharge and charge state, respectively (Figure 3a). Formation of Li_2O_2 is confirmed by XRD after the 1st discharge (Figure 3b). The APNC-3 cathode having a high macropore volume, shows a specific discharge capacity of ~1800 mAh/g already without optimization of secondary parameters. APNC-1, having the lowest macropore volume, shows under the same conditions a specific discharge capacity of ~900 mAh/g (Figure 3a). If we analyze in more detail the discharge process, the APNC-3 cathode starts the formation of Li_2O_2 (= $O_2 + 2Li^+ + 2e^- \rightarrow Li_2O_2$) from 2.67 V vs. Li/Li^+ and exhibits an average discharge overpotential (η_{dis}) of 0.29 V, while the APNC-1 cathode can drive the Li_2O_2 formation starting from 2.60 V vs. Li/Li^+ and shows an η_{dis} of 0.39 V vs. Li/Li^+ (Table 2 and Supporting Figure S4). For the recharge reaction (= $Li_2O_2 \rightarrow O_2 + 2Li^+ + 2e^-$), the APNC-3 cathode can start the reaction at 3.0 V vs. Li/Li^+ and show an average recharging overpotential (η_{cha}) of 0.45 V, while the APNC-1 cathode starts the recharge reaction from 3.17 V vs. Li/Li^+ with an overpotential of 0.61 V (Table 2 and Supporting Figure S5).

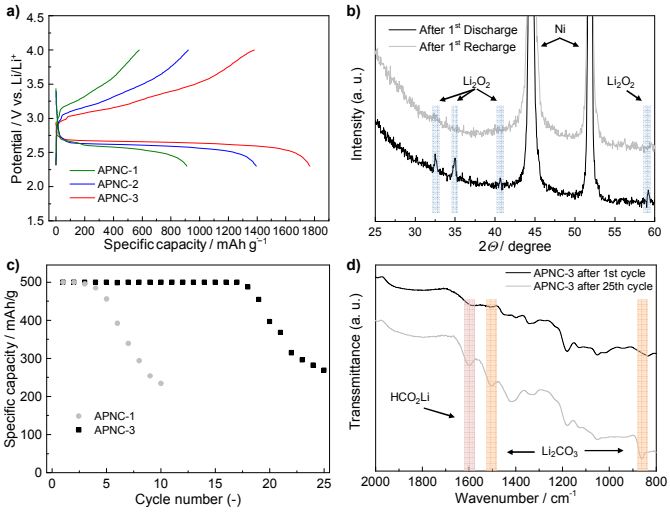

Figure 3. (a) Charge-discharge curves of APNCs. (b) ex-situ XRD for APNC-3 after 1st discharge and recharge. (c) Cycle performance of APNC-1 and APNC-3. (d) Ex-situ FTIR spectra for APNC-3 after 1st cycle and 25th cycle.

Table 2. Electrochemical properties of APNCs.

Cathode	Q_{dis} (mAh/g)	Q_{rec} (mAh/g)	Q_{rec}/Q_{dis}	η_{dis} (V)	η_{rec} (V)
APNC-1	912	579	0.64	0.39	0.61
APNC-2	1394	921	0.66	0.37	0.49
APNC-3	1767	1380	0.78	0.29	0.45

The value given by Q_{rec}/Q_{dis} at the 1st cycle characterizes the general loss for the conditioning/formation of the solid electrolyte interface and is another measure for the quality and inert ness of the electrode. (note that the later Coulombic efficiency is much higher, as expected for a real battery system). The APNC-3 cathode shows a Q_{rec}/Q_{dis} of 0.78 while the APNC-1 cathode possess 0.64, which means that the APNC-3 cathode relies on less reactions with the Li system to turn electrochemically stable (Table 2). These results experimentally confirm that a theoretical study showing pore structure takes a very important enrolment during electrochemical redox reactions related to oxygen at cathode.[5] Charge-discharge cycling while limiting the specific loading capacity to 500 mAh/g while applying more harsh 250 mA/g of current density was carried out to check the relation of pore structure and cycling performance by using APNC-1 and APNC-3 (Figure 3c). As the results, we found that the APNC-3 cathode has a longer cycling stability compared to the APNC-1 cathode. It is noted that these results on the rechargebility and cycling performance are still affected by the side reactions and degradation of Li metal anode caused by exposure to oxygen[36] , i.e. the degradation is not only due to the cathode, but also due to the suboptimal anode design and solvent/salt effects. Future engineering works on cell configuration is certainly necessary to lever the real potential of noble carbon cathodes. Previous theoretical researches in this battery system suggested that the pore structure of a cathode have a stronger effect on electrochemical performance in this system: Pore blocking may be a reason for rate as well as capacity limitation since insulating Li_2O_2 or side products forms on the surface of porous carbon and cap the pores.[5] This results in passivating the carbon and/or blocking the oxygen supply to the catalytic carbon surface. Actually, the electronic conductivity could decrease dramatically even after monolayer deposition of Li_2O_2.[37] In addition, there is a deposition of side products, such as Li_2CO_3, during charge-discharge reactions.[34] We could confirm the formation of Li_2CO_3 and side products after the 25th cycle (Figure 3d).

Table 3. Comparison of rechargebility for a various of carbon-based cathodes.

Cathode	Q_{rec}/Q_{dis}	Q_{dis} (mAh/g)	Q_{rec} till 4.0 V vs. Li/Li^+ (mAh/g)	I (mA/g)	Electrolyte	Anode	S_{BET} (m^2/g)	Ref.
APNC-3	0.78	1767	1380	100	1M LiTFSI in TEGDME	Li metal	1476	This work
XC-72	0.67	300	~200	400	1M LiTFSI in DME	Li metal	Typically ~250	35
Carbon	0.62	900	566	70	0.5M $LiPF_6$ in TEGDME	$LiFePO_4$	150	34
GNSs	0.47	2359	~1100	50	1M $LiClO_4$ in PC	Li metal	309	39
VA-NCCF	0.25	40000	~10000	500	1M LiTFSI in TEGDME	Li metal	-	40
N-CNT	0	900	0	75	1M LiPF6 in EC/PC (1:1)	Li metal	41	38

A comparison of the rechargebility of APNC-3 with previous research results using carbon-based cathodes is shown in Table 3.[29, 35, 38-40] As we already mentioned above, the specific capacity obtained above 4.0 V vs. Li/Li^+ contains the irreversible capacity from the electrolyte decomposition.[8, 37] Therefore, we only compared the specific capacity in these data until 4.0 V vs. Li/Li^+ to assess a more comparable electrochemical performance of the cathodes at the recharging reaction (= OER; $Li_2O_2 \rightarrow O_2 + 2Li^+ + 2e^-$). From this comparison, it is shown that APCN-3 is up to now one of the best performing carbon-based cathodes used in RLOB. For example, a carbon-nanotube-based cathode showed no performance as it cannot

start the recharging reaction below 4.0 V vs. Li/Li^+, due to missing electrocatalytic performance.

Conclusions

In conclusion, we delineated a successful synthesis of a high performance and affordable Adenosine-derived noble carbon cathode for LOBs with bifunctional electrocatalytic activity and showed that the pore structure of APNC is a key feature to control the electrochemical performance of this electrochemical system. Pore structure of APNCs is tuned by amount of salt, thereby producing highly N-doped porous carbons with different meso- and macropore volume. Such a pore structure successfully minimizes the influence of the discharge product Li_2O_2 or side products on the electrode performance. We demonstrated a favourable electrochemical performance of the optimized cathode with less side reaction by operating the cell below 4.0 V vs. Li/Li^+ at the recharging reaction. From this results and our previous report,[27] a noble nitrogen-doped porous carbon possessing a high surface area together with large-scale accessible porosity would be the best carbon-based cathode for Li-O2 battery system. Although porous Au still outperforms APNC cathodes, we believe that a sustainable and affordable character is necessary within the development of real life, scalable battery systems.

Acknowledgement

K.S. is indebted to Max Planck Society. We thank for Mr. Jaeho Kim (Seoul National University) for the XPS and Raman spectroscopy measurements. The technical staffs are acknowledged for standard analysis.

Notes and references

[a] Max Planck Institute of Colloids and Interfaces, Colloid Chemistry Department, Am Mühlenberg 1 OT Golm, D-14476 Potsdam, Germany.
‡ Current occupation: National Institute for Materials Science (NIMS), International Center for Materials Nanoarchitectonics (MANA), 1-1 Namiki, Tsukuba, 305-0044 Ibaraki, Japan.
*E-mail:sakaushi.ken@nims.go.jp

Electronic Supplementary Information (ESI) available: Synthesis, XPS, Raman, TEM and supplementary electrochemical characterization data. See DOI: 10.1039/c000000x/

1. M. S. Dresselhaus and I. L. Thomas, *Nature*, 2001, **414**, 332-337.
2. B. Dunn, H. Kamath and J.-M. Tarascon, *Science*, 2011, **334**, 928-935.
3. IEA, *World Energy Outlook 2014*, IEA, 2014.
4. G. Girishkumar, B. McCloskey, A. C. Luntz, S. Swanson and W. Wilcke, *J. Phys. Chem. Lett.*, 2010, **1**, 2193.
5. J. Christensen, P. Albertus, R. S. Sanchez-Carrera, T. Lohmann, B. Kozinsky, R. Liedtke, J. Ahmed and A. Kojic, *J. Electrochem. Soc.*, 2011, **159**, R1.
6. Y.-C. Lu, B. M. Gallant, D. G. Kwabi, J. R. Harding, R. R. Mitchell, M. S. Whittingham and Y. Shao-Horn, *Energy Environ. Sci.*, 2013, **6**, 750.
7. C. O. Laoire, S. Mukerjee, K. M. Abraham, E. J. Plichta and M. A. Hendrickson, *J. Phys. Chem. C*, 2010, **114**, 9178.
8. B. D. McCloskey, R. Scheffler, A. Speidel, D. S. Bethune, R. M. Shelby and A. C. Luntz, *J. Am. Chem. Soc.*, 2011, **133**, 18038.
9. L. Johnson, C. Li, Z. Liu, Y. Chen, S. A. Freunberger, P. C. Ashok, B. B. Praveen, K. Dholakia, J.-M. Tarascon and P. G. Bruce, *Nat. Chem.*, 2014, **6**, 1091.
10. N. B. Aetukuri, B. D. McCloskey, J. M. Garcia, L. E. Krupp, V. Viswanathan and A. C. Luntz, *Nat. Chem.*, 2015, **7**, 50.
11. L. Zhao, L.-Z. Fan, M.-Q. Zhou, H. Guan, S. Qiao, M. Antonietti and M.-M. Titirici, *Adv. Mater.*, 2010, **22**, 5202.
12. K. Sakaushi, G. Nickerl, F. M. Wisser, D. Nishio-Hamane, E. Hosono, H. Zhou, S. Kaskel and J. Eckert, *Angew. Chem. Int. Ed.*, 2012, **51**, 7850.
13. N. Brun, K. Sakaushi, L. Yu, L. Giebeler, J. Eckert and M. M. Titirici, *Phys. Chem. Chem. Phys.*, 2013, **15**, 6080.
14. K. Sakaushi, E. Hosono, G. Nickerl, T. Gemming, H. Zhou, S. Kaskel and J. Eckert, *Nat. Commun.*, 2013, **4**, 1485.
15. J. Liu, T. Yang, D.-W. Wang, G. Q. Lu, D. Zhao and S. Z. Qiao, *Nat. Commun.*, 2013, **4**.
16. H.-W. Liang, Z.-Y. Wu, L.-F. Chen, C. Li and S.-H. Yu, *Nano Energy*, 2015, **11**, 366.
17. G. Ertl, *Angew. Chem. Int. Ed.*, 2008, **47**, 3524.
18. J. Sauer and H.-J. Freund, *Catal. Lett.*, 2014, **145**, 109.
19. J. P. Paraknowitsch and A. Thomas, *Energy Enviro. Sci.*, 2013, **6**, 2839.
20. K. Sakaushi and M. Antonietti, *Bull. Chem. Soc. Jpn*, 2015, **88**, 386.
21. M. Glerup, M. Castignolles, M. Holzinger, G. Hug, A. Loiseau and P. Bernier, *Chem. Commun.*, 2003, 2542.
22. F. Jaouen, M. Lefèvre, J.-P. Dodelet and M. Cai, *J. Phys. Chem. B*, 2006, **110**, 5553.
23. R. Liu, D. Wu, X. Feng and K. Müllen, *Angew. Chem. Int. Ed.*, 2010, **49**, 2565.
24. J. P. Paraknowitsch, J. Zhang, D. Su, A. Thomas and M. Antonietti, *Adv. Mater.*, 2010, **22**, 87.
25. W. Yang, T.-P. Fellinger and M. Antonietti, *J. Am. Chem. Soc.*, 2010, **133**, 206.
26. N. Ranjbar Sahraie, J. P. Paraknowitsch, C. Göbel, A. Thomas and P. Strasser, *J. Am. Chem. Soc.*, 2014, **136**, 14486.
27. K. Sakaushi, T. P. Fellinger and M. Antonietti, *ChemSusChem*, 2015, 8, 1156.
28. Z. Peng, S. A. Freunberger, Y. Chen and P. G. Bruce, *Science*, 2012, **337**, 563.
29. M. M. Ottakam Thotiyl, S. A. Freunberger, Z. Peng and P. G. Bruce, *J. Am. Chem. Soc.*, 2013, **135**, 494.
30. J. Lu, Y. Lei, K. C. Lau, X. Luo, P. Du, J. Wen, R. S. Assary, U. Das, D. J. Miller, J. W. Elam, H. M. Albishri, D. A. El-Hady, Y.-K. Sun, L. A. Curtiss and K. Amine, *Nat. Commun.*, 2013, **4**, 2383.
31. D. M. Itkis, D. A. Semenenko, E. Y. Kataev, A. I. Belova, V. S. Neudachina, A. P. Sirotina, M. Hävecker, D. Teschner, A. Knop-Gericke, P. Dudin, A. Barinov, E. A. Goodilin, Y. Shao-Horn and L. V. Yashina, *Nano Lett.*, 2013, **13**, 4697.
32. N. Fechler, T.-P. Fellinger and M. Antonietti, *Adv. Mater.*, 2013, **25**, 75.
33. Y. Ren, Z. Ma, R. E. Morris, Z. Liu, F. Jiao, S. Dai and P. G. Bruce, *Nat. Commun.*, 2013, **4**, 2015.
34. B. D. McCloskey, D. S. Bethune, R. M. Shelby, G. Girishkumar and A. C. Luntz, *J. Phys. Chem. Lett.*, 2011, **2**, 1161.
35. B. D. McCloskey, D. S. Bethune, R. M. Shelby, T. Mori, R. Scheffler, A. Speidel, M. Sherwood and A. C. Luntz, *J. Phys. Chem. Lett.*, 2012, **3**, 3043.
36. J. Hassoun, H.-G. Jung, D.-J. Lee, J.-B. Park, K. Amine, Y.-K. Sun and B. Scrosati, *Nano Lett.*, 2012, **12**, 5775.
37. B. D. McCloskey, A. Speidel, R. Scheffler, D. C. Miller, V. Viswanathan, J. S. Hummelshøj, J. K. Nørskov and A. C. Luntz, *J. Phys. Chem. Lett.*, 2012, **3**, 997.
38. Y. Li, J. Wang, X. Li, J. Liu, D. Geng, J. Yang, R. Li and X. Sun, *Electrochem. Commun.*, 2011, **13**, 668.
39. B. Sun, B. Wang, D. Su, L. Xiao, H. Ahn and G. Wang, *Carbon*, 2012, **50**, 727.
40. J. Shui, F. Du, C. Xue, Q. Li and L. Dai, *ACS Nano*, 2014, **8**, 3015.

TOC

A pore structure of cathode is an essence to control the electrochemical performance of lithium-O_2 battery system.